

# Strain distributions in quantum dots of arbitrary shape

A. D. Andreev,<sup>a)</sup> J. R. Downes, D. A. Faux, and E. P. O'Reilly  
*Department of Physics, University of Surrey, Guildford GU2 5XH, United Kingdom*

(Received 5 November 1998; accepted for publication 30 March 1999)

A method based on the Green's function technique for calculating strain in quantum dot (QD) structures has been developed. An analytical formula in the form of a Fourier series has been obtained for the strain tensor for arrays of QDs of arbitrary shape taking into account the anisotropy of elastic properties. Strain distributions using the anisotropic model for semiconductor QDs are compared to results of a simplified model in which the elastic properties are assumed to be isotropic. It is demonstrated that, in contrast to quantum wells, both anisotropic and isotropic models give similar results if the symmetry of the QD shape is less than or equal to the cubic symmetry of the crystal. The strain distribution for QDs in the shape of a sphere, cube, pyramid, hemisphere, truncated pyramid, and flat cylinder are calculated and analyzed. It is shown that the strain distributions in the major part of the QD structure are very similar for different shapes and that the characteristic value of the hydrostatic strain component depends only weakly on the QD shape. Application of the method can considerably simplify electronic structure calculations based on the envelope function method and plane wave expansion techniques. © 1999 American Institute of Physics. [S0021-8979(99)06713-4]

## I. INTRODUCTION

In recent years, research interest into semiconductor structures containing zero-dimensional objects (quantum dots, QDs) has increased considerably. From the point of view of fundamental science, QDs provide an opportunity to study new physical effects arising from the three-dimensional (3D) confinement of the carriers. On the practical side, semiconductor heterostructures containing QDs have a wide range of potential applications as new or improved optoelectronic devices such as QD lasers, creating a demand for the development of fast and reliable methods for modeling their physical properties. In most cases, QD structures are fabricated with an intrinsic elastic strain field arising from the lattice mismatch between the QD and matrix material (for example, Ref. 1). Knowledge of this strain field is crucial for further device modeling since the strain substantially modifies the electronic band structure which, in turn, strongly affects the performance of optoelectronic devices.<sup>2,3</sup>

The calculation of the intrinsic strain field requires solving a 3D problem in elasticity theory for the nontrivial geometry of the QD shape. Commonly used methods for the solution of this problem are finite-difference methods<sup>4,5</sup> and atomistic techniques.<sup>6</sup> These methods require much computation time and computer memory. A simple and elegant method for calculating strain fields due to a single *isotropic* QD of arbitrary shape was presented by Downes *et al.*<sup>7</sup> as a simplification of the work of Eshelby.<sup>8</sup> This method provides *analytic* solutions for simple geometries such as cubic dots or pyramidal dots,<sup>9</sup> and numerical solutions for more complex geometries, but neglects anisotropy.

Most semiconductor compounds crystallize in the zincblende structure, giving cubic crystals. The elastic properties of a cubic crystal are anisotropic. The anisotropy coefficient, defined in terms of the elastic constants as  $(C_{11} - C_{12})/2C_{44}$ , is typically equal to 0.5 in III-V semiconductors, compared to the isotropic value of 1. The sensitivity of some physical properties to strain suggests that anisotropic effects could be important in semiconductor materials and that an isotropic approximation may be poor, particularly in certain crystallographic directions. On the other hand, for two-dimensional problems in which isotropic and anisotropic solutions are compared, the isotropic approximation appears to be very good which suggests that it is generally not necessary to perform the more complex calculation.<sup>10</sup> No similar comparison has been reported for QDs.

In this article, we present an original method based on the Green's function technique for the calculation of strain distributions in QD structures. While the real-space Green's function in the isotropic limit has been known for some time, the calculation of the elastic Green's function for anisotropic cubic crystals has proved more challenging.<sup>11,12</sup> Our method takes account of the anisotropy of the elastic properties in cubic crystals and produces a nearly analytical solution for the strain field due to QDs of arbitrary shape. We study the influence of the QD shape on the strain distribution and the applicability of the isotropic approximation for QD structures.

The article is organized as follows. In the next section, we derive a general analytical formula for the Fourier transform of the strain tensor for QDs of arbitrary shape. The QD shape enters only through the Fourier transform of the QD characteristic function which can be found analytically in most cases (expressions for the sphere, cube, hemisphere, pyramid, cylinder, cone, and truncated pyramid are presented in the Appendix). At the end of this section, we present a

<sup>a)</sup>On leave from A.F. Ioffe Physical-Technical Institute, 26 Polytekhnicheskaya, St.-Petersburg 194021, Russia; electronic mail: a.andreev@surrey.ac.uk

straightforward expression for crystals with cubic symmetry. We then treat the case of cubic crystals in detail in Sec. III, where we compare the results of the isotropic model with the full anisotropic treatment for cubic crystals. It is demonstrated that, despite the relatively strong anisotropy in the elastic properties of semiconductor crystals, the results can be very similar in both cases. In Sec. IV, we study the influence of the QD shape on the strain distribution by comparing results for the sphere, cube, hemisphere, pyramid, truncated pyramid and flat cylinder. Finally, in Sec. V, we summarize the results and present the conclusions. We note that by including sufficient terms, the Fourier series can be summed to calculate the real space strain distribution to any desired level of accuracy. Of equal or greater importance, the technique is also particularly well-suited as input to electronic structure calculations based on the envelope function method and using a plane-wave expansion technique, because the strain-dependent matrix element linking any pair of plane waves can be determined analytically.

## II. THE GREEN'S FUNCTION METHOD FOR THE CALCULATION OF STRAIN

The Green's tensor  $G_{ln}(\mathbf{r})$  gives the displacement at  $\mathbf{r}$  in the direction  $l$  due to a unit point force in direction  $n$  placed at the origin. The Green's tensor for infinite anisotropic elastic media<sup>13</sup> is the solution of the equation,

$$\lambda_{iklm} \frac{\partial G_{ln}(\mathbf{r})}{\partial x_k \partial x_m} = -\delta(\mathbf{r}) \delta_{in} \quad (1)$$

with the boundary condition  $G_{ln}(\mathbf{r}) \rightarrow 0$  as  $|\mathbf{r}| \rightarrow \infty$ . In Eq. (1),  $\mathbf{r}=(x_1, x_2, x_3)$  is the space coordinate and  $\lambda_{iklm}$  is the tensor of elastic moduli. Here and below, we use the usual rule for summation over 1,2,3 for repeating indices unless the sum is indicated explicitly. In this article, as a first approximation, we assume that the Green's tensor is the same for the matrix and QD material. If necessary, the different elastic moduli can be considered as a perturbation.

To solve Eq. (1) and find  $G_{ln}(\mathbf{r})$ , we use a Fourier transform technique. For the Fourier transform of the Green's tensor,  $\tilde{G}_{ln}(\boldsymbol{\xi})$ , we obtain from Eq. (1) the following linear equation:

$$\lambda_{iklm} \xi_k \xi_m \tilde{G}_{ln}(\boldsymbol{\xi}) = \frac{\delta_{in}}{(2\pi)^3}. \quad (2)$$

The method of inclusions as proposed by Eshelby<sup>8</sup> is used to find the strain distribution in the QD structure. The displacement in a structure with a single QD can be expressed as the convolution of the Green's tensor and the forces spread over the QD surface,

$$u_i^s(\mathbf{r}) = u_i^T \chi_{\text{QD}}(\mathbf{r}) + \int G_{in}(\mathbf{r}-\mathbf{r}') \sigma_{nk}^T dS'_k, \quad (3)$$

where  $\chi_{\text{QD}}(\mathbf{r})$  is the characteristic function of the QD, equal to unity within the QD and zero outside;  $\sigma_{nk}^T = \lambda_{nkpr} e_{pr}^T$  and  $\sigma_{nk}^T$ ,  $e_{pr}^T$  and  $u_i^T$  are the components of the stress and strain tensors and the displacement caused by the "initial" strain due to the lattice mismatch. The superscript "s" indicates that this expression refers to a single QD.

The integration in Eq. (3) is carried out over the QD surface. Using Gauss's theorem, the strain tensor in a single QD structure is given by

$$e_{ij}^s(\mathbf{r}) = e_{ij}^T \chi_{\text{QD}}(\mathbf{r}) + \frac{1}{2} \int_{\text{QD}} \left[ \frac{\partial G_{in}(\mathbf{r}-\mathbf{r}')}{\partial x_j \partial x_k} + \frac{\partial G_{jn}(\mathbf{r}-\mathbf{r}')}{\partial x_i \partial x_k} \right] \times \lambda_{nkpr} e_{pr}^T dV', \quad (4)$$

where integration is carried out over the QD volume. Using the convolution theorem and then taking the Fourier transform gives

$$\tilde{e}_{ij}^s = e_{ij}^T \tilde{\chi}_{\text{QD}}(\boldsymbol{\xi}) - \frac{(2\pi)^3}{2} \{ \xi_i \tilde{G}_{jn}(\boldsymbol{\xi}) + \xi_j \tilde{G}_{in}(\boldsymbol{\xi}) \} \times \lambda_{nkpr} \xi_k e_{pr}^T \tilde{\chi}_{\text{QD}}(\boldsymbol{\xi}), \quad (5)$$

where  $\tilde{\chi}_{\text{QD}}(\boldsymbol{\xi})$  is the Fourier transform of the QD characteristic function. Equation (5) gives the general expression for the Fourier transform of the strain tensor in a structure containing a single QD of arbitrary shape. This is a general formula valid for crystals of cubic or any other symmetry. Note that the QD shape enters only as the Fourier transform of the QD characteristic function.

The elastic problem is a linear one and so the solution for a QD array is obtained as a superposition of the elastic fields for single QDs, namely,

$$e_{ij} = \sum_{n_1, n_2, n_3} e_{ij}^s(x_1 - n_1 d_1, x_2 - n_2 d_2, x_3 - n_3 d_3), \quad (6)$$

where  $d_1, d_2, d_3$  are the periods in the  $x, y$  and  $z$  directions, respectively. An additional condition for  $e_{ij}$  arises from the requirement of minimum elastic energy for the periodic QD array. Equivalently, the strain tensor averaged over the elementary 3D superlattice unit cell is zero ( $\overline{e_{ij}} = 0$ ). From Eq. (6) it follows that the coefficients for the Fourier series expansion of  $e_{ij}$  are equal to  $[(2\pi)^3 / (d_1 d_2 d_3)] \tilde{e}_{ij}^s(\boldsymbol{\xi}_n)$ , where  $\boldsymbol{\xi}_n = 2\pi(n_1/d_1, n_2/d_2, n_3/d_3)$ . Finally, therefore, for the strain tensor in a QD array we obtain

$$e_{ij} = \frac{(2\pi)^3}{d_1 d_2 d_3} \sum_{n_1, n_2, n_3} \tilde{e}_{ij}^s(\boldsymbol{\xi}_n) \exp(i \boldsymbol{\xi}_n \cdot \mathbf{r}), \quad (7)$$

where the summation is carried out over all values of  $n_1, n_2, n_3$ , except the case when  $n_1 = n_2 = n_3 = 0$ .

We now treat the specific case of crystals with cubic symmetry. Here, the tensor of the elastic moduli has three independent components and can be represented in the form

$$\lambda_{iklm} = C_{12} \delta_{ik} \delta_{lm} + C_{44} (\delta_{il} \delta_{mk} + \delta_{im} \delta_{kl}) + C_{an} \sum_{p=1}^3 \delta_{ip} \delta_{kp} \delta_{lp} \delta_{mp}, \quad (8)$$

where  $C_{11}, C_{12}, C_{44}$  are the elastic moduli and  $C_{an} = C_{11} - C_{12} - 2C_{44}$  describes the anisotropic part of the tensor. In the isotropic limit,  $C_{an} = 0$  and the elastic moduli coincide with the isotropic Lamé constants  $C_{12} = \lambda$  and  $C_{44} = \mu$ .

Substituting Eq. (8) into Eq. (2), we find that the expression for  $\tilde{G}_{ln}(\boldsymbol{\xi})$  has the form

$$\sum_l \{(C_{12} + C_{44})\xi_i \xi_l + C_{44} \delta_{il} \xi^2 + C_{an} \delta_{il} \xi_i^2\} \tilde{G}_{ln}(\xi) = \frac{\delta_{in}}{(2\pi)^3}. \quad (9)$$

Introducing the ‘‘scalar’’ product  $(\xi \tilde{G})_n \equiv \xi_i \tilde{G}_{ln}(\xi)$ , Eq. (9) becomes

$$\tilde{G}_{in}(\xi) = \frac{\delta_{in} / (2\pi)^3 - (C_{12} + C_{44}) \xi_i (\xi \tilde{G})_n}{C_{44} \xi^2 + C_{an} \xi_i^2}. \quad (10)$$

Multiplying Eq. (9) by  $1/\xi_i$ , performing the summation over  $i$  and rearranging for  $(\xi \tilde{G})_n$  yields

$$(\xi \tilde{G})_n = \frac{1}{(2\pi)^3} \frac{\xi_n}{C_{44} \xi^2 + C_{an} \xi_n^2} \times \left\{ 1 + (C_{12} + C_{44}) \sum_{p=1}^3 \frac{\xi_p^2}{C_{44} \xi^2 + C_{an} \xi_p^2} \right\}^{-1}. \quad (11)$$

Combining Eq. (10) and Eq. (11), the expression for the Fourier transform of the Green’s tensor for crystals with cubic symmetry is obtained,

$$\tilde{G}_{in}(\xi) = \frac{1}{(2\pi)^3} \frac{\delta_{in}}{C_{44} \xi^2 + C_{an} \xi_i^2} - \frac{1}{(2\pi)^3} \frac{(C_{12} + C_{44}) \xi_i \xi_n}{(C_{44} \xi^2 + C_{an} \xi_i^2)(C_{44} \xi^2 + C_{an} \xi_n^2)} \times \left\{ 1 + (C_{12} + C_{44}) \sum_{p=1}^3 \frac{\xi_p^2}{C_{44} \xi^2 + C_{an} \xi_p^2} \right\}^{-1}. \quad (12)$$

The Green’s function tensor can be found, in principle, by performing the inverse Fourier transform with the corresponding integral evaluated using the spherical coordinate system and the residue theorem.<sup>13</sup> In the case  $C_{an} = 0$ , Eq. (12) reduces to the well-known isotropic result.<sup>8</sup>

The strain tensor may be obtained by substituting Eq. (12) into Eq. (5). For cubic crystals, the initial strain is

$$e_{ij}^T = \frac{a_M - a_{QD}}{a_{QD}} \delta_{ij} \equiv \epsilon_0 \delta_{ij}, \quad (13)$$

where  $a_M$  and  $a_{QD}$  are the lattice constants of the matrix and the QD materials, respectively. Combining this with the explicit expression for the elastic tensor we find  $\lambda_{nkpr} e_{pr}^T = \epsilon_0 (C_{11} + 2C_{12}) \delta_{nk}$  and Eq. (5) is simplified for cubic crystals to

$$\tilde{e}_{ij}^s = \epsilon_0 \tilde{\chi}_{QD}(\xi) \times \left\{ \delta_{ij} - \frac{(2\pi)^3}{2} (C_{11} + 2C_{12}) [\xi_i (\xi \tilde{G})_j + \xi_j (\xi \tilde{G})_i] \right\}. \quad (14)$$

Using the explicit expression for  $(\xi \tilde{G})_i$ , the final formula for the Fourier transform of the strain tensor for QDs with cubic symmetry is obtained,

$$\tilde{e}_{ij}^s(\xi) = \epsilon_0 \tilde{\chi}_{QD}(\xi) \left\{ \delta_{ij} - \frac{(C_{11} + 2C_{12}) \xi_i \xi_j / \xi^2}{1 + (C_{12} + C_{44}) \sum_{p=1}^3 \frac{\xi_p^2}{C_{44} \xi^2 + C_{an} \xi_p^2}} \times \frac{1}{2} \left[ \frac{1}{C_{44} + C_{an} \xi_i^2 / \xi^2} + \frac{1}{C_{44} + C_{an} \xi_j^2 / \xi^2} \right] \right\}. \quad (15)$$

In the form of the Fourier series, this formula and Eq. (7) give analytical expressions for the strain distribution in structures containing QDs of arbitrary shape. The QD shape enters in Eq. (15) only in the form of the Fourier transform  $\tilde{\chi}_{QD}(\xi)$  of the QD characteristic function. Analytical expressions for  $\tilde{\chi}_{QD}(\xi)$  for different shapes (sphere, cube, hemisphere, cylinder, cone, pyramid, truncated pyramid) are given in the Appendix. Note that Eq. (15) simplifies considerably in the isotropic approximation. Inserting  $C_{an} = 0$ , we obtain

$$\tilde{e}_{ij}^{iso}(\xi) = \epsilon_0 \tilde{\chi}_{QD}(\xi) \left( \delta_{ij} - \frac{3\lambda + 2\mu}{\lambda + 2\mu} \frac{\xi_i \xi_j}{\xi^2} \right), \quad (16)$$

where  $\lambda = C_{12}$  and  $\mu = C_{44}$  are the Lamé constants for an isotropic elastic medium. From this equation, we immediately find that the hydrostatic component of the strain tensor,  $e_{ii}^{iso} \equiv e_h$ , is constant inside the QD and zero outside in the isotropic approximation and given by

$$e_{ii}^{iso} = \epsilon_0 \frac{4\mu}{\lambda + 2\mu} \chi_{QD}(\mathbf{r}). \quad (17)$$

Thus, the deviation of the hydrostatic strain from this constant value is characteristic of the influence of elastic anisotropy on the strain distribution in QD structures.

All calculations presented in the following sections assume that the elastic constants of the dot and matrix are the same and equal to those of the matrix. It is possible, however, to treat the difference of the elastic moduli as a perturbation. In this case the Fourier transform of the elastic tensor is represented in the form  $\tilde{e}_{ij} = \tilde{e}_{ij}^{(0)} + \tilde{e}_{ij}^{(1)} + \tilde{e}_{ij}^{(2)} + \dots$ , where  $\tilde{e}_{ij}^{(0)}$  is the strain tensor calculated using elastic constants equal to those of the matrix [Eq. (15)],  $\tilde{e}_{ij}^{(N)} \propto \delta \lambda^N$  is the  $N$ th correction of the perturbation series, and  $\delta \lambda \sim (\delta \lambda)_{iklm} \equiv \lambda_{iklm}^{QD} - \lambda_{iklm}^M$  is the difference of the elastic constants between the QD material and the matrix material. The  $N$ th correction,  $\tilde{e}_{ij}^{(N)}$ , of this perturbation series can be expressed as the convolution of the  $(N - 1)$ -th correction with the characteristic function  $\tilde{\chi}_{QD}$ , providing a convenient and fast iteration scheme to find the elastic strain with required accuracy.

There are also arguments for choosing the elastic constants of the matrix for both matrix and the dots as outlined in an earlier publication.<sup>15</sup> First, the elastic constants of a semiconductor alloy are not generally known and interpolating between binaries, for example, may not necessarily yield accurate elastic constants for a ternary alloy. Second, the elastic constants of a material in a state of high strain may also differ from those of the relaxed material, leading to further uncertainties as to the best choice of elastic constants. Finally, Keyes<sup>16</sup> showed that, to a very good approximation,

TABLE I. Elastic moduli for some III–V semiconductors (see Ref. 14) (in units of  $10^{11}$  Pa).  $C_{an}$  is the measure of the elastic anisotropy.

Material	$C_{11}$	$C_{12}$	$C_{44}$	$C_{an}$
GaAs	1.18	0.54	0.59	-0.54
InAs	0.83	0.45	0.40	-0.42
InSb	0.66	0.36	0.30	-0.30
GaSb	0.88	0.40	0.43	-0.38

the elastic constants in most III–V semiconductors depend chiefly on the nearest-neighbor lattice spacing and he proposed an empirical scaling relationship. Experimental results on the quaternary alloy GaInAsP have supported Keyes' scaling rule.<sup>17</sup> For strained QD structures, the Keyes scaling relationship suggests that it is most appropriate to choose the elastic constants of the *barrier* material for *all* materials in the system because, prior to the relaxation of the misfit strain, all materials possess the same lattice spacing.

### III. ANISOTROPIC AND ISOTROPIC MODELS

For cubic crystals, the degree of elastic anisotropy can be characterized by the magnitude of the anisotropic part,  $C_{an} = C_{11} - C_{12} - 2C_{44}$ , of the elastic tensor. If  $C_{an} = 0$ , we have the isotropic limit and when  $C_{an}$  is comparable with other elastic moduli, the elastic properties are strongly anisotropic. Elastic constants for some III–V binaries are listed in the Table I. From this table it follows that the elastic anisotropy in III–V semiconductor compounds is rather strong since the anisotropic part of the elastic tensor is  $|C_{an}| \sim C_{12} \sim C_{44}$ . For example, the effective Poisson's ratio varies from  $\nu \approx 1/3$  for the (001) direction to  $\nu \approx 1/5$  for the (111) direction. This variation can result in a significant dependence of strain on the space direction. This is best illustrated for strained quantum wells (QWs) where the strain depends strongly on the direction of the normal to the QW plane, which in turn affects the position of the energy levels of the carriers localized in the QWs.<sup>18</sup>

It is natural to expect, therefore, that the elastic anisotropy of III–V compounds is an important factor in determining the strain distribution in QD structures. However, we demonstrate in this section that this is not generally the case. In most cases, the elastic anisotropy gives a rather small correction to the results of the isotropic approximation. Qualitatively this fact can be explained as follows. In contrast to the QW structures, the strain distribution in QD structures is determined by two physically different factors: first, the degree of symmetry of the QD shape and, second, the anisotropy of the elastic properties.

Three separate cases can now be identified: (i) the QD shape has higher symmetry than the cubic symmetry of the elastic properties; (ii) the QD shape has cubic symmetry; and (iii) the symmetry of the QD shape is less than the cubic symmetry of the elastic properties. In the first case, the anisotropy in the strain distribution is caused largely by the anisotropy of the elastic properties. Therefore, the isotropic and anisotropic models can give different results. On the other hand, in most cases when the symmetry of the QD shape is less than or equal to the cubic symmetry, the domi-

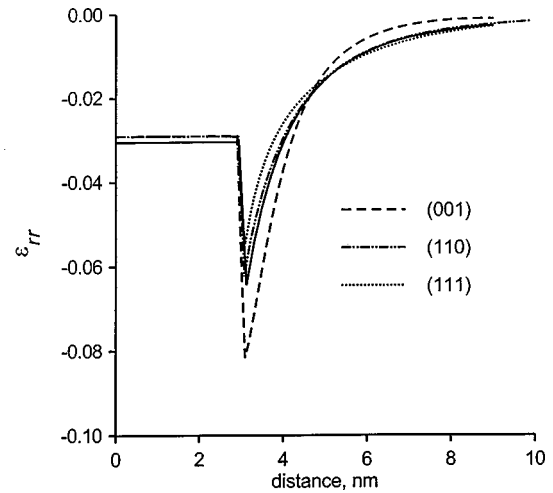


FIG. 1. Radial strain tensor component,  $e_{rr}$ , for different directions through a spherical dot is presented for the isotropic (solid line) and anisotropic (dashed and dotted lines) models. The radius of the QD is 3 nm and the origin of the coordinate system is at the QD center. Parameters for GaAs (see Table I) have been used and the misfit strain is  $-6.7\%$ .

nant contribution to the anisotropy of the strain distribution is caused by the ‘‘anisotropy’’ of the QD shape rather than by the anisotropy of the elastic properties. Therefore, the isotropic assumption yields results which reproduce the main features of the fully anisotropic model. To demonstrate this point, we have performed calculations of the strain distribution for the sphere, cube and the pyramid. Elastic constants for GaAs, as presented in Table I, are used for all calculations presented in this and the following section. The misfit strain,  $\epsilon_0$ , is  $-0.067$  corresponding to InAs dots contained in a GaAs matrix and, for the isotropic calculations,  $C_{12} = 0.54 \times 10^{11}$  Pa and  $C_{44} = 0.59 \times 10^{11}$  Pa are used with  $C_{an} = 0$ .

The strain distribution is itself isotropic for an isotropic spherical QD. The degree of anisotropy induced by the cubic symmetry of the elastic properties can be characterized by the radial component of the strain tensor in spherical coordinates,  $e_{rr}$ , which is plotted for three directions in Fig. 1. Inside the QD the isotropic and anisotropic models give constant strain with a value which is nearly identical for both models. Outside the QD the results of the two models are different. Along the (001) direction, the change in  $e_{rr}$  is greater for the anisotropic model than for the isotropic model and the maximum value of  $|e_{rr}|$  is  $\sim 30\%$  larger. The reverse situation occurs along the (111) direction. Here, the maximum value of  $|e_{rr}|$  is less for the anisotropic model than for the isotropic model. Along the (110) direction the results of the two models nearly coincide. Thus, for a spherical QD, the influence of the elastic anisotropy is very small inside the sphere, while outside the dot this influence is rather large in the (100) direction and small in the (110) direction. Outside the dot the isotropic model effectively gives the strain distribution averaged over different directions.

The comparison of the anisotropic and isotropic models for the cubic QD is presented in Fig. 2. Here, the symmetry of the QD is the same as the symmetry of the elastic properties. Therefore, the influence of the elastic anisotropy is

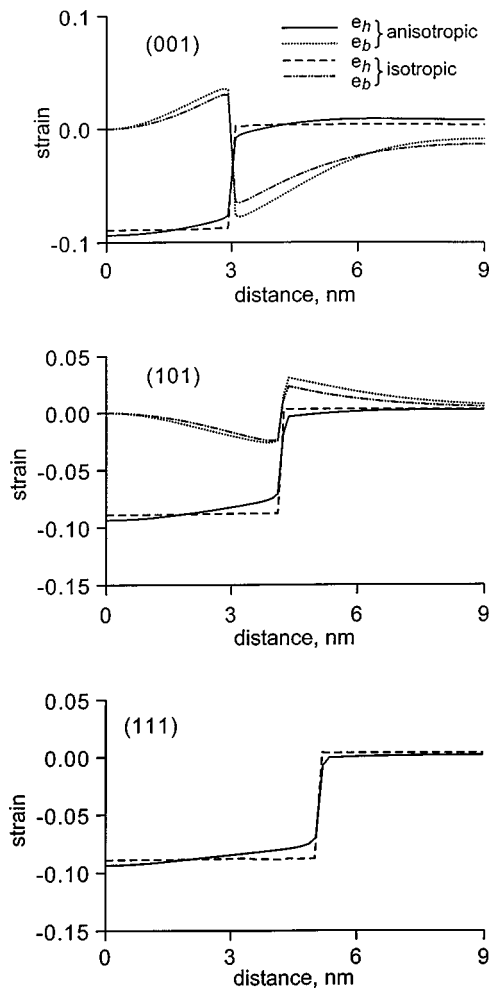


FIG. 2. Hydrostatic,  $e_h$ , and biaxial,  $e_b$ , strain components along selected directions for a cubic dot of length 6 nm are presented for the isotropic and anisotropic models. The origin of the coordinate system is at the QD center. Parameters for GaAs have been used and the misfit strain is  $-6.7\%$ .

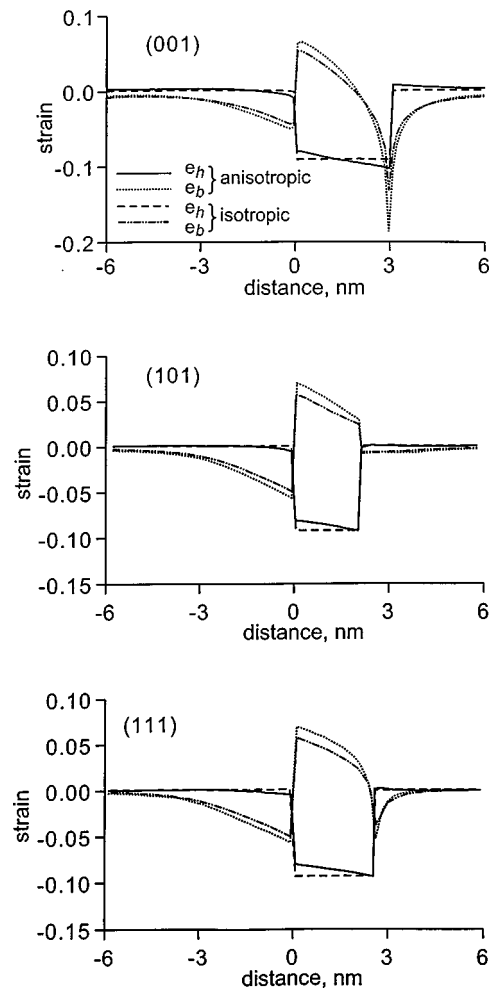


FIG. 3. Hydrostatic,  $e_h$ , and biaxial,  $e_b$ , strain components along selected directions for a pyramidal dot of base length 6 nm and height 3 nm are presented for the isotropic and anisotropic models. The base sides are parallel to the  $x$  and  $y$  axes and the origin of the coordinate system is at the center of the base. Parameters for GaAs have been used and the misfit strain is  $-6.7\%$ .

much smaller than for the spherical QD. The maximum difference between the anisotropic and isotropic models again occurs along (001), analogous to the case of the sphere. However, in the cubic QD  $|(e_{ij}^{iso} - e_{ij}^{aniso})/e_{ij}^{iso}| \leq 10\%$  for the (001) direction and less than 5%–7% for other directions.

For the pyramid, the symmetry of the QD shape is less than the cubic symmetry of the elastic properties. Again one can see that the results of the anisotropic and isotropic models are very similar qualitatively and quantitatively. In contrast to the spherical QD, the difference between the two models is less outside the pyramidal QD than inside it.

In the previous section we showed that, in the isotropic limit, the hydrostatic strain component  $e_h = e_{ii}$  is a constant inside the QD and zero outside. For the anisotropic model, the component  $e_h$  has a weak spatial dependence (see Figs. 2 and 3). In the case of the cube,  $e_h$  is large in the center of the QD and decreases slightly away from the QD center. For the pyramid,  $e_h$  increases in the direction from the pyramid center to the top of the pyramid. However, the dependence of  $e_h$  on position is rather weak, reflecting our conclusion that the influence of elastic anisotropy on QD strain distributions is relatively small.

#### IV. INFLUENCE OF THE QD SHAPE ON THE STRAIN DISTRIBUTION

QDs of different shape can be fabricated by controlling the material and growth conditions. The shape of fabricated QDs is, however, not known accurately<sup>19</sup> and therefore it is important to study the influence of the QD shape on the strain field. It is clear that the strain tensor will be different at least in the areas where the QD shapes do not match, but are there characteristics of the strain field which are similar in QDs of different shape? To answer this question we compare the strain distribution in the sphere, cube, pyramid, hemisphere, truncated pyramid and flat cylinder. Again elastic constants for GaAs are used,  $\epsilon_0 = -0.067$  and, for the isotropic calculations, explicit values of  $C_{12}$  and  $C_{44}$  are used with  $C_{an} = 0$ .

Figure 4 shows a contour plot of the radial component of the stress tensor for the sphere and cube calculated for the isotropic model. In contrast to the sphere, the cube has sharp edges and so near these edges, as well as inside the QD, the stress distribution is different between the two cases. But

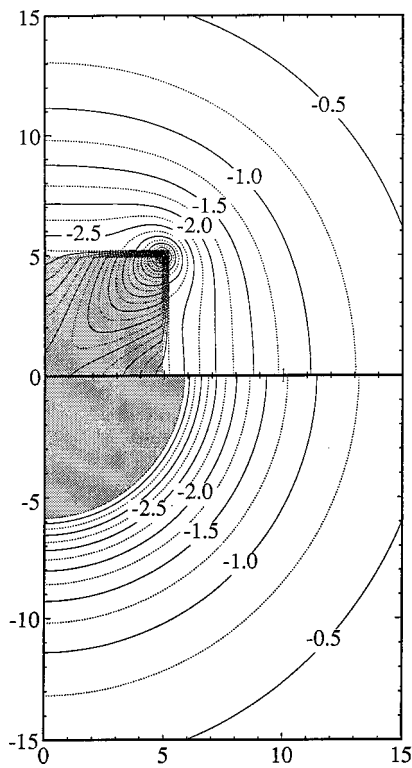


FIG. 4. Radial strain component,  $\epsilon_{rr}$ , surrounding a spherical and cubic inclusion with equal volume. The cube sides are of length 10 in arbitrary units and the sphere has a radius of  $(750/\pi)^{1/3}$ . The calculation uses the isotropic approximation. Parameters for GaAs have been used and the misfit strain is  $-6.7\%$ .

outside the QD, the stress contours become very similar for the cube and sphere. For distances of the order of the QD size the stress distributions outside the dot become independent of the QD shape. The stress contours for the cube become spherical and nearly coincide with those of the sphere.

Let us now consider the anisotropic model and focus on the hydrostatic strain component,  $e_h = e_{ii}$ , and the biaxial strain component,  $e_b = e_{zz} - (e_{xx} + e_{yy})/2$ . These strain components define the potential profile for the electrons and the splitting of the light and heavy hole states, respectively. Figure 5 shows the dependence of  $e_h$  and  $e_b$  for the spherical and cubic QDs in the (001), (110) and (111) directions. In spite of the fact that the stress distribution inside the QD for the sphere and cube is different, the characteristic value of the hydrostatic strain component is very close for the two shapes. This means that the barrier height for electrons has a comparatively weak dependence on the QD shape. Along the (110) and (111) directions the QD sizes are different and therefore  $e_h$  drops to zero at different positions. The biaxial strain,  $e_b$ , for the two shapes is different near the QD boundary. Along the (001) direction  $e_b$  is large inside the cube and smaller outside compared to the sphere. The reverse situation arises along (110); inside the cube  $e_b$  is smaller, while outside it is larger. For both shapes, along the (111) direction, the biaxial strain is zero due to symmetry.

A comparison of the strain distribution for the pyramid and hemisphere is presented in Fig. 6. The hydrostatic strain is similar for both shapes throughout most of the QD, similar to the case of the cube and sphere. In the lower part of the

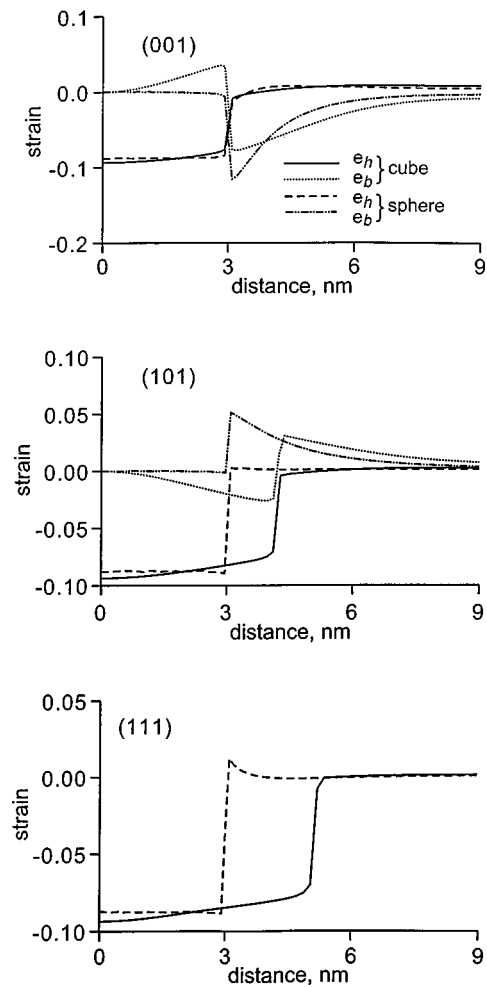


FIG. 5. Hydrostatic,  $e_h$ , and biaxial,  $e_b$ , strain components along selected directions for a spherical and cubic dot are presented for the anisotropic model. The radius of the spherical dot is 3 nm and the length of the cubic dot is 6 nm. The origin of the coordinate system is at the center of the dots. Parameters for GaAs have been used and the misfit strain is  $-6.7\%$ .

pyramid and hemisphere,  $e_h$  and  $e_b$  are nearly identical, but in the upper part the strain is different due to the sharp edges of the pyramid and smooth boundary of the hemisphere. In particular, in the (001) direction, the pyramid has a sharp corner which results in a steep variation of the biaxial strain. A similar effect can be seen in the (111) direction near the pyramid edge. However, compared to the (001) direction, the change in biaxial strain is not so steep because along the (111) direction the pyramid edge forms a sharp angle in one direction only, while the top of the pyramid forms a sharp angle in two directions. In the (111) direction the biaxial strain in the hemisphere has no extremum near the upper boundary and its variation is qualitatively the same as the sphere or cube along the (001) or (110) direction. The behavior of the biaxial strain suggests a general rule: near sharp boundaries (edges or corners) the biaxial strain varies steeply and has an extremum.

Figure 7 shows the shear strain tensor components for the pyramid and hemisphere. For  $z < 0$ , the shear components are effectively identical and along the (001) direction the shear components are zero due to symmetry. In the (101) direction, the only nonzero shear component is  $e_{xz}$ . In this

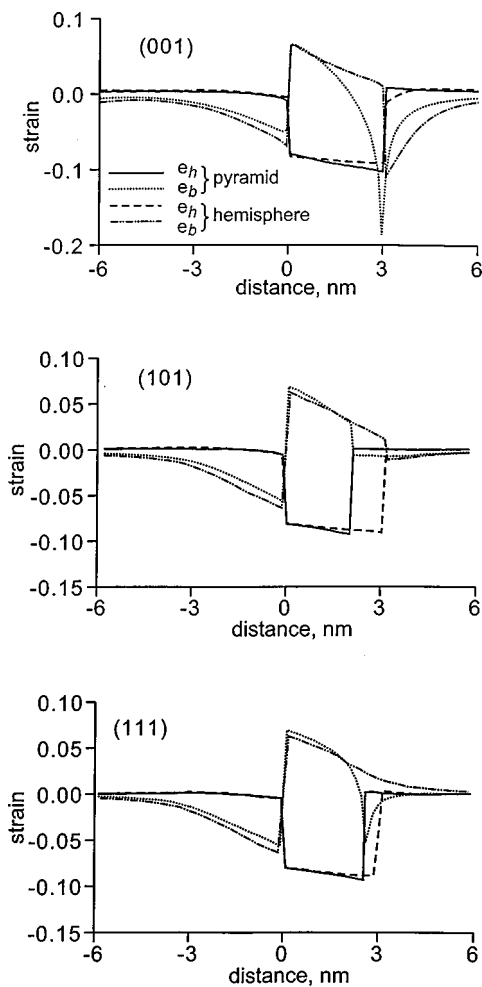


FIG. 6. Hydrostatic,  $e_h$ , and biaxial,  $e_b$ , strain components along selected directions for a hemispherical and a pyramidal dot are presented for the anisotropic model. The hemisphere radius is 3 nm and the pyramid has a base length of 6 nm and height 3 nm. The origin of the coordinate system is at the center of the dots. Parameters for GaAs have been used and the misfit strain is  $-6.7\%$ .

direction, the variation of  $e_{xz}$  for the two shapes is qualitatively similar, but for the pyramid the amplitude of the jump near the QD boundary is larger than that for the hemisphere. Along the (111) direction all three shear components are non-zero and  $e_{xz} = e_{yz}$ . In this direction, the pyramid has a sharp edge, therefore these strain components for the pyramid vary more steeply near the QD boundary.

The hydrostatic and biaxial strain for the cylinder and truncated pyramid are presented in Fig. 8. Along the (001) direction  $e_h$  and  $e_b$  are very close for the two shapes, except in a small area outside the dot near the boundary where  $|e_b|$  for the truncated pyramid is larger. In the QD plane [directions (100) and (110)], the truncated pyramid and cylinder have different sizes. Therefore, the hydrostatic component drops to zero at different positions, but again the characteristic value of  $e_h$  is nearly equal for these two shapes. Also note that in the QD plane the strain components outside the dot vanish over a distance of the order of a quarter of the QD diameter or base length. This is much more rapid than in the (001) direction or for “nonflat” shapes (sphere, cube or

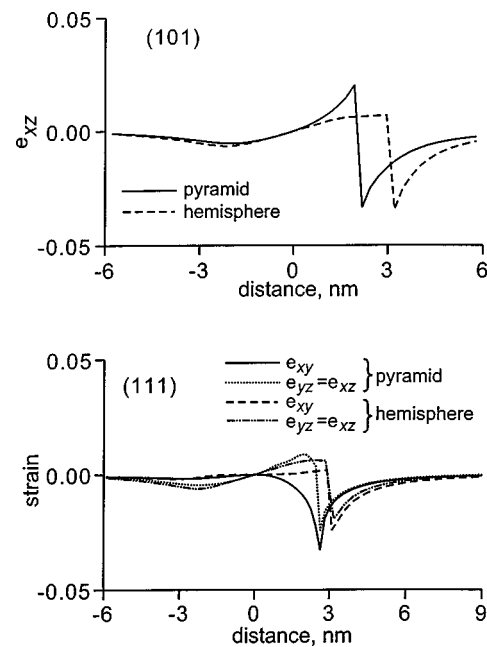


FIG. 7. Shear strain components for a hemispherical and a pyramidal dot are presented for the anisotropic model. The hemisphere radius is 3 nm and the pyramid has a base length of 6 nm and height 3 nm. The origin of the coordinate system is at the center of the dots. Parameters for GaAs have been used and the misfit strain is  $-6.7\%$ .

hemisphere), where the strain vanishes over distances of the order of the QD size along the corresponding direction.

### V. CONCLUSIONS

In this article, we have presented a new method based on a Green’s function approach to calculate strain distributions in QDs of arbitrary shape. Our general method includes elastic anisotropy in full with specific results for cubic crystals presented as a special case. The advantage of this method is that it enables nearly analytical expressions for the strain distribution to be obtained in the form of a Fourier series and the calculation is therefore much faster than other numerical methods. It becomes particularly effective for the calculation of the strain distribution for periodic arrays, QD superlattices or vertically coupled QDs. In these cases, the Fourier series converges quickly and so fewer Fourier components are required in order to obtain accurate results. The other advantage of our method is that the QD shape enters only through the Fourier transform of the QD characteristic function (a 3D analogue of the 1D Heaviside function), which is calculated analytically for all common QD shapes.

The calculation method is also particularly well suited as an input step in calculations of the electronic properties of quantum dots. Most calculations of confined state energies in quantum dots have used the envelope function method, with the wave functions calculated using a basis of plane wave states. Previous studies have often included two large integration steps in calculating the matrix element linking any pair of plane wave states. Firstly, the real-space strain field is calculated explicitly throughout the structure. This real-space strain field is then used as input in a second integration step to determine the strain-related contributions to the inter-

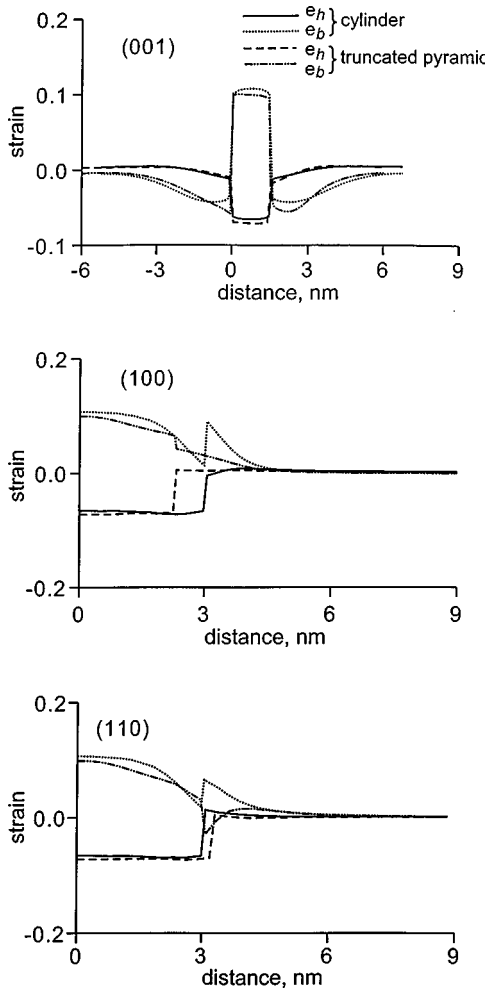


FIG. 8. Hydrostatic,  $e_h$ , and biaxial,  $e_b$ , strain components along selected directions for a truncated pyramid and a cylindrical dot are presented for the anisotropic model. The pyramid base length is 6 nm, the width of the top face is 3 nm and its height is 1.5 nm. The diameter and height of the cylinder are 6 nm and 1.5 nm, respectively. The origin of the coordinate system is at the center of the dots. Parameters for GaAs have been used and the misfit strain is  $-6.7\%$ .

plane-wave matrix elements. By contrast, using the analysis presented here, each of these matrix elements can be determined analytically, being proportional to a single term in the Fourier series we have introduced.

Comparing the results of the simplified isotropic model and the anisotropic model reveals that, in contrast to the QW case, the two models generally give very similar results. The elastic properties have cubic symmetry while, in most cases, the QD shape has lower symmetry. Therefore, the anisotropy of the strain distribution is mainly determined by the anisotropy of the QD shape rather than by the anisotropy of the elastic properties of the media. Therefore, for QDs, anisotropic and isotropic models give very similar results for strain distributions. We have also calculated and compared strain distributions in different QD shapes and found that the characteristic values of the hydrostatic strain component depend only weakly on the QD shape. Strain distribution for structures with different shapes are qualitatively similar throughout most of the QD. Differences mainly arise from the sharp edges and corners of some shapes when compared

to the smooth boundaries of others. Outside the dot, strain distributions become nearly independent of the QD shape over distances of the order of the QD size. Finally, we note that at present the dimensions of QDs are uncertain to at least 10% and so the isotropic approximation should suffice, but as technology improves and the shape and size of QDs becomes known to a greater precision, anisotropic calculations may become necessary to accurately determine the strain distributions.

## ACKNOWLEDGMENTS

The visit of ADA to University of Surrey was supported by a grant from the Royal Society and JRD was supported by the Engineering and Physical Sciences Research Council (UK) under Grant No. GR/K 81447.

## APPENDIX

The Fourier transform of the characteristic function is a 3D integral

$$\tilde{\chi}_{\text{QD}}(\xi) = \int_{\text{QD}} e^{-i\xi \cdot \mathbf{r}} dV, \quad (\text{A1})$$

where the integration is carried out over the QD volume. For most QD shapes, the function  $\tilde{\chi}_{\text{QD}}(\xi)$  can be found analytically. In this section, we present formulas for the sphere, cube, pyramid, cylinder, hemisphere, cone and truncated pyramid.

For a sphere centered at the origin,

$$\tilde{\chi}_{\text{QD}}(\xi) = \frac{4\pi}{\xi} \left[ \frac{\sin(\xi R)}{\xi^2} - \frac{R \cos(\xi R)}{\xi} \right], \quad (\text{A2})$$

where  $R$  is the sphere radius.

For the cuboid,

$$\tilde{\chi}_{\text{QD}}(\xi_n) = \frac{8}{\xi_1 \xi_2 \xi_3} \sin(\xi_1 a_1/2) \sin(\xi_2 a_2/2) \sin(\xi_3 a_3/2), \quad (\text{A3})$$

where  $a_1$ ,  $a_2$ ,  $a_3$  are the cuboid dimensions and the origin of the coordinates is at the center of the QD.

For the pyramid,

$$\begin{aligned} \tilde{\chi}_{\text{QD}}(\xi_n) = & \chi_1(\xi_1, \xi_2, \xi_3, L_x, L_y) + \chi_1(\xi_2, \xi_1, \xi_3, L_y, L_x) \\ & + \chi_1(-\xi_1, \xi_2, \xi_3, L_x, L_y) \\ & + \chi_1(-\xi_2, \xi_1, \xi_3, L_y, L_x), \end{aligned} \quad (\text{A4})$$

with

$$\begin{aligned} \chi_1(\xi_1, \xi_2, \xi_3, L_x, L_y) = & \frac{1}{\xi_2 \xi_3} \left\{ e^{-i\xi_3 h} \left[ I_{e0} \left( \frac{L_x}{2}, -\xi_1 + \xi_3 \frac{L_y}{L_x} + \xi_2 \frac{2h}{L_x} \right) \right. \right. \\ & \left. \left. - I_{e0} \left( \frac{L_x}{2}, -\xi_1 - \xi_3 \frac{L_y}{L_x} + \xi_2 \frac{2h}{L_x} \right) \right] \right. \\ & \left. - I_{e0} \left( \frac{L_x}{2}, -\xi_1 + \xi_2 \frac{L_y}{L_x} \right) + I_{e0} \left( \frac{L_x}{2}, -\xi_1 - \xi_2 \frac{L_y}{L_x} \right) \right\}, \end{aligned} \quad (\text{A5})$$



where  $L_x$  and  $L_y$  are the pyramid base dimensions (the base is assumed to form a rectangle),  $h$  is the pyramid height,  $I_{e0}(a, \xi) = [e^{i\xi a} - 1]/(i\xi)$ , the origin of the coordinate system is at the center of the base and the  $x$  and  $y$  axes are parallel to the base sides.

For the cylinder,

$$\tilde{\chi}_{\text{QD}}(\xi_n) = \frac{2\pi D}{\xi_{\parallel} \xi_3} \sin(\xi_3 h/2) J_1\left(\frac{D \xi_{\parallel}}{2}\right), \quad (\text{A6})$$

where  $J_1$  is a Bessel function,  $h$  is the cylinder height,  $D$  is the diameter and the origin of the coordinate system is at the center of the cylinder.

For the hemisphere,

$$\tilde{\chi}_{\text{QD}}(\xi) = \frac{1}{2} \tilde{\chi}_{\text{QD}}^{\text{sphere}}(\xi) + \frac{2\pi i}{\xi_3} \left[ \frac{R}{\xi_{\parallel}} J_1(R \xi_{\parallel}) - R^2 I_{j0}(R \xi_3, R \xi_{\parallel}) \right], \quad (\text{A7})$$

where  $\tilde{\chi}_{\text{QD}}^{\text{sphere}}$  is the Fourier transform for the sphere,  $R$  is the hemisphere radius,  $\xi_{\parallel} = \sqrt{\xi_1^2 + \xi_2^2}$  and  $I_{j0}$  denotes the integral

$$I_{j0}(\alpha, \beta) = \int_0^1 x \cos(\alpha \sqrt{1-x^2}) J_0(\beta x) dx, \quad (\text{A8})$$

where  $J_0$  is a Bessel function. The integral in Eq. (A8) is best calculated numerically.

For the cone,

$$\tilde{\chi}_{\text{QD}}(\xi) = \frac{2\pi i}{\xi_z} \left[ e^{-i\xi_z h} I_2(\xi_{\parallel} R, \xi_z h) - \frac{R}{\xi_{\parallel}} J_1(\xi_{\parallel} R) \right], \quad (\text{A9})$$

where  $R$  is the radius of the cone base,  $h$  is the cone height and  $I_2$  denotes the integral

$$I_2(\alpha, \beta) = \int_0^1 x J_0(\alpha x) e^{i\beta x} dx. \quad (\text{A10})$$

This integral can be expressed as a power series or calculated numerically.

For the truncated pyramid,

$$\tilde{\chi}_{\text{QD}}(\xi) = \tilde{\chi}_{\text{QD}}^{\text{PYR}}(\xi, L_x^b, L_y^b, h_l) - e^{-i\xi_z h_t} \tilde{\chi}_{\text{QD}}^{\text{PYR}}(\xi, L_x^t, L_y^t, h_s), \quad (\text{A11})$$

where  $L_x^b$  and  $L_y^b$  are the base lengths,  $L_x^t$  and  $L_y^t$  are the dimensions of the truncated face,  $h_t$  is the height,  $\tilde{\chi}_{\text{QD}}^{\text{PYR}}(\xi, L_1, L_2, h)$  is the Fourier transform for a pyramid with base lengths  $L_1$  and  $L_2$  and height  $h$ ;  $h_s = L_x^t h_t / (L_x^b - L_x^t)$  and  $h_l = L_x^b h_t / (L_x^b - L_x^t)$ . In the above formula, the origin of the coordinate system is at the center of the QD base.

<sup>1</sup>Y. Androussi, A. Lefebvre, B. Courboulès, N. Grandjean, J. Massies, T. Bouhacina, and J. P. Aimé, *Appl. Phys. Lett.* **65**, 1162 (1994).  
<sup>2</sup>E. P. O'Reilly, *Semicond. Sci. Technol.* **4**, 121 (1989).  
<sup>3</sup>E. P. O'Reilly and A. R. Adams, *IEEE J. Quantum Electron.* **30**, 366 (1994).  
<sup>4</sup>M. Grundmann, O. Stier, and D. Bimberg, *Phys. Rev. B* **52**, 11969 (1995).  
<sup>5</sup>T. Benabbas, P. François, Y. Androussi, and A. Lefebvre, *J. Appl. Phys.* **80**, 2763 (1996).  
<sup>6</sup>M. A. Cusack, P. R. Briddon, and M. Jaros, *Phys. Rev. B* **54**, R2300 (1996).  
<sup>7</sup>J. R. Downes, D. A. Faux, and E. P. O'Reilly, *J. Appl. Phys.* **81**, 6700 (1997).  
<sup>8</sup>J. D. Eshelby, *Proc. R. Soc. London, Ser. A* **241**, 376 (1957).  
<sup>9</sup>G. Pearson, A. D. Andreev, D. A. Faux, and E. P. O'Reilly (unpublished).  
<sup>10</sup>D. A. Faux and J. Haigh, *J. Phys.: Condens. Matter* **2**, 10289 (1990).  
<sup>11</sup>P. H. Dederichs and G. Leibfried, *Phys. Rev.* **188**, 1175 (1969).  
<sup>12</sup>T. Mura and N. Kinoshita, *Phys. Status Solidi B* **47**, 607 (1971).  
<sup>13</sup>I. M. Lifshits and L. N. Rosentsverg, *Zh. Eks. Teor. Fiz.* **17**, 9 (1947) (in Russian) [*Sov. Phys. JETP*].  
<sup>14</sup>M. P. C. M. Krijn, *Semicond. Sci. Technol.* **6**, 27 (1991).  
<sup>15</sup>J. R. Downes, D. A. Faux, and E. P. O'Reilly, *J. Appl. Phys.* **82**, 3754 (1997).  
<sup>16</sup>R. W. Keyes, *J. Appl. Phys.* **33**, 3371 (1962).  
<sup>17</sup>A. D. Prins and D. J. Dunstan, *Philos. Mag. Lett.* **58**, 37 (1988).  
<sup>18</sup>C. G. Van de Walle, *Phys. Rev. B* **39**, 1871 (1989).  
<sup>19</sup>H. Lee, R. Lowe-Webb, W. Yang, and P. C. Sercel, *Appl. Phys. Lett.* **72**, 812 (1998).